euspen's 16th International Conference & Exhibition, Nottingham, UK, May 2016
www.euspen.eu

Characterisation of a scintillation flat panel detector employed by an X-ray computed tomography system: measurements of MTF, NPS and DQE

Wenjuan Sun[1], Anastasios Konstantinidis[2], Ilias Billas[1], Michael McCarthy[1], Stephen Brown[1],Hannah Corcoran[1,3]

[1]*National Physical Laboratory, Hampton Road, Teddington, TW11 0LW, United Kingdom*
[2]*Christie NHS Foundation Trust, Manchester, M20 4BX, United Kingdom*
[3]*University College London, London, WC1E 6BT, United Kingdom*

Email: wenjuan.sun@npl.co.uk

Abstract
The physical performance of a flat panel X-ray detector when used as an integrated component of an X-ray computed tomography (XCT) system, is highly important when data captured from it are used for three-dimensional metrology purposes. Recent trends in the development of XCT systems for dimensional measurements, for both industrial and medical applications, require high speed detectors with high image quality, high dynamic range and the ability to function over a large area. However, the development of robust performance evaluation techniques for detectors used for dimensional metrology is still in its infancy. In this study, an example scintillation detector employed by an XCT system is characterised from 70 kV to 150 kV in terms of modulation transfer function, noise power spectrum and detective quantum efficiency. Experimental results are presented and discussed.

Keywords: X-ray computed tomography, detector, characterisation, DQE, MTF, NPS

1. Introduction

A scintillation detector is an advanced X-ray registration device that indirectly converts X-ray photons into digital signals. It consists of a scintillator to convert X-rays to visible light and a digital sensor to convert visible light to digital signal [1]. Due to their merits of high performance over large dynamic range and active area [2], scintillation detectors are widely used in XCT for both medical and industrial applications. However, the quality of scintillation detectors depends on the manufacturing technology employed, which can significantly affect the overall performance of an XCT system. In this study, the detective quantum efficiency (DQE), recommended by the IEC 62220-1 standard [3], was used to evaluate the performance of a scintillation flat panel detector of an industrial XCT system[4] .

2. Detective quantum efficiency

The DQE describes the ability of an X-ray detector to transfer the signal-to-noise ratio (SNR) from the radiation field to the resulting digital image[3]. DQE is calculated from equation (1) [5], where pMTF is the averaged (over horizontal and vertical orientations of the detector) pre-sampling modulation transfer function, K_a is the measured air kerma at the detector surface, $\frac{\Phi}{K_a}$ is the incoming fluence per exposure ratio [6] and $NNPS(f)$ is the averaged normalised noise power spectrum (NPS). Further details of how to perform DQE tests can be found in the literatures [7, 8] .

$$DQE(u,v) = \frac{pMTF^2(f)}{\frac{\Phi}{K_a}K_a \cdot NNPS(f)} \quad (1)$$

2.1 Air kerma at detector surface

K_a is the energy transferred from initial particles (X-rays in this case) to charged particles in air per unit mass (given in gray (Gy)). It can be measured using an ionisation chamber. With the known distances between the X-ray source to the ionisation chamber and the source to the detector, the air kerma at the detector surface can then be derived using the inverse square law to correct for the distance.

2.2 Fluence per exposure ratio

The ratio $\frac{\Phi}{K_a}$ expresses the relationship between X-ray photon fluence (in X-rays per square millimetre) and K_a [6]. For a polychromatic X-ray source, it is calculated based on the used X-ray spectrum with the monochromatic $\frac{\Phi}{K_a}$ (tabulated data). To estimate the X-ray spectrum, the Half Value Layer (HVL), which is the thickness of an absorbing material (aluminium in our case) that reduces half of the input K_a, is required.

With the HVL, the X-ray spectral shape for given irradiation conditions (i.e. tube voltage, external filtration, measured HVL and anode angle) can be calculated using a spectra simulator (i.e. SpekCalc in this case [9]).

2.3 Pre-sampling modulation transfer function

The pMTF quantifies the spatial resolution of an imaging system. The pMTF can be calculated using either the edge method or the slit method [7, 8, 10]. It was decided to use the edge method for this study as it leads to more accurate results and edge test objects are widely available.

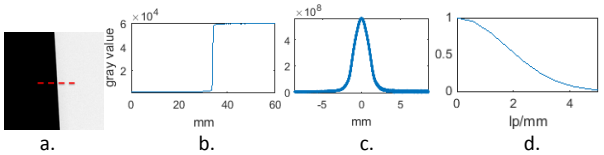

a. b. c. d.

Figure 1. pMTF calculation. a. X-ray image of slanted edge sample, b. ESF, c. LSF, d. pMTF. lp/mm is line pairs per millimetre.

To test the pMTF of an X-ray detector, an edge sample, a high purity (99.9 %) tungsten (W) thin plate (1 mm thickness in our case) with polished edge and surface, can be used. The edge

sample was placed directly on top of the detector surface with a shallow angle between the edge and the row or column of the detector pixel array. The image of the slanted edge was taken to produce the edge spread function (ESF) and the ESF was then differentiated to get the line spread function (LSF). Finally, the modulus of the Fourier transform (FT) of the LSF, pMTF, was normalized to 1 at 0 spatial frequency (see Figure 1 and equation (2)).

$$pMTF(x) = |FT\{LSF(x)\}| = \left|FT\{\frac{d}{dx}[ESF(x)]\}\right| \quad (2)$$

2.4 Noise power spectrum

The NPS describes the spectral decomposition of the noise variance as a function of spatial frequency. It is the modulus of the Fourier transform of the noise auto-covariance function [3]. The calculation of NPS is shown in equation (3), where $I(x,y)$ corresponds to the data within the regions of interest (ROIs) of the flat images, $S(x,y)$ is a second order polynomial fit of $I(x,y)$ to remove low frequency background trends (such as heel effect), Δx and Δy are pixel pitches in horizontal and vertical orientations, u and v are the corresponding spatial frequencies for both orientations, N_x and N_y are the number of pixels of the used ROIs (256 x 256 in this case) and M is the total number of ROIs used to extract the final NPS. It is recommended that the total number of pixels should be at least four million to provide a precise estimate of the NPS value (i.e. with a confidence level of 95 %). Therefore, a number of flat images may be required. The detailed procedure can be found in [3].

$$NPS(u,v) = \frac{\Delta x \cdot \Delta y}{M \cdot N_x \cdot N_y} \sum_{m=1}^{M} \left| \sum_{i=1}^{N_x} \sum_{j=1}^{N_y} FT\left\{ I\left(x_{m,i}, y_{m,j}\right) - S\left(x_{m,i}, y_{m,j}\right) \right\} \right|^2 \quad (3)$$

3. Instrumentations

The X-ray detector under investigation is a scintillation flat panel detector. It consists of a thallium doped cesium iodide (CsI:TI) scintillator, coupled to an amorphous silicon (a-Si) thin film transistor (TFT) sensor. The detector has 2000 × 2000 pixels with a pixel size of 200 µm × 200 µm and a total area of 40 cm × 40 cm. The detector is part of an industrial XCT system that employs a polychromatic X-ray cone-beam source [4]. The maximum energy of the X-ray source is 225 kV. The X-ray detector was tested at 70 kV, 90 kV, 120 kV and 150 kV, which are within the typical energy range of the system. An exposure time of 1 second was used to represent the most common setting of the XCT system.

4. Results and discussion

The pMTF, NNPS and DQE parameters were calculated as a function of spatial frequency up to the Nyquist frequency. The results of pMTF and DQE are shown in Figure 2 and Figure 3 respectively.

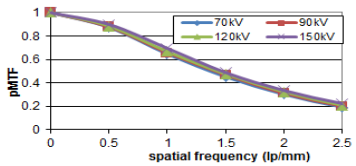

Figure 2. pMTF of the detector.

It can be seen from the results that the differences between the values of pMTF at different energies are negligible. This happens because all the mean energies of the used X-ray spectra were higher than 50 keV, i.e. higher than the K-absorption edges of I (33.2 keV) and Cs (36.0 keV) that constitute the CsI:Tl scintillator. The DQE results in Figure 3 show the efficiency of the detector as a function of spatial frequency, detector air kerma level and X-ray energy. It should be noted that the DQE values decrease as a function of spatial frequency due to the increased noise effect at higher frequencies. Furthermore, the DQE values are slightly lower for low K_a values due to the increased effect of the digital sensor's electronic noise. However, for higher K_a values the DQE results reach a plateau which corresponds to a linear and quantum-limited behaviour. Finally, the DQE values decrease as a function of energy, due to the decreased absorption of X-rays from the scintillator at higher energy levels. The maximum DQE (at 0.5 lp/mm) was around 0.6 which demonstrates a good performance of the investigated flat panel detector.

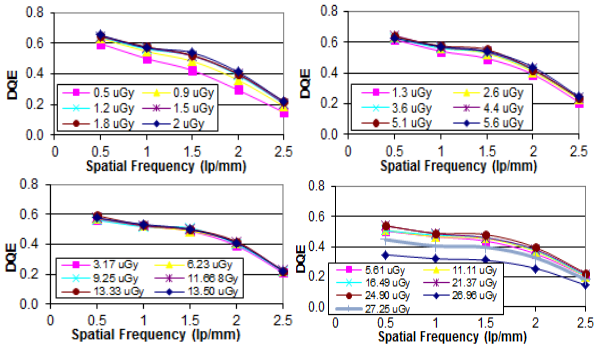

Figure 3. DQE results of the scintillation detector at 70 kV (top-left), 90 kV (top-right), 120 kV (bottom-left) and 150 kV (bottom-right).

5. Conclusions

This paper demonstrates the evaluation of a scintillation detector of an XCT system using DQE as recommended by the IEC 62220-1 standard [3]. The two important parameters, MTF and NPS, reveal the spatial resolution and the noise level of the detectors and DQE shows how efficiently signal and noise can be transferred through a detector with respect to spatial frequency. Both MTF and DQE (around 0.6 maximum) results demonstrate the good performance of the detector over a range of energies (from 70 kV to 150 kV). Future work should consider how DQE can be used in the performance evaluation of detectors for XCT systems, where volume data are reconstructed from thousands of images.

It should be noted that the lag effect has not been considered in this study. All tests images were taken with a reasonable time gap of at least 5 second between each image to reduce the impact of image lag. However, the image lag issue will be further investigated in the future.

References

[1] Nikl M 2006 *Meas. Sci. Technol.* **17** 37-54
[2] Konstantinidis A C, et al. 2013 *IEEE Trans. Nucl. Sci.* **60** 3969-80
[3] IEC 62220-1 2003 International Electrotechnical Commission
[4] Sun W, Brown S B and Leach R K 2012 NPL Report ENG 32
[5] Beutel J, Kundel H L and Metter R L V 2000 *Handbook of Medical Imaging. Volume 1. Physics and psychophysics* (SPIE) p949
[6] Boone J M 1998 *Proc. of Proc. of SPIE* Vol3336 pp592-601
[7] Samei E, Flynn M J and Reimann D A 1998 *Med, Phys.* **25** 102-13
[8] Buhr E and Neitzel S G n-K a U 2003 *Med, Phys.* **30** 2323-31
[9] Poludniowski G, Landry G, DeBlois F, Evans P M and Verhaegen F SpekCalc: a program to calculate photon spectra from tungsten anode x-ray tubes 7
[10] Fujita H, Tsai D-Y, Itoh T, Doi K, Morishita J, Ueda K and Ohtsuka A 1992 *IEEE Trans. Med. Imag.* **11** 34-39